

Low pressure line shape study of nitrogen-perturbed acetylene transitions in the $\nu_1 + \nu_3$ band over a range of temperatures¹

Chad Povey, Mileno Guilloré Obregon, Adriana Predoi-Cross, Sergey V. Ivanov, Oleg G. Buzykin, and Franck Thibault

Abstract: Six nitrogen-perturbed transitions of acetylene within the $\nu_1 + \nu_3$ absorption band have been recorded using a three-channel diode laser spectrometer. The goal being an improved understanding of both broadening and narrowing effects of low-pressure acetylene under the influence of nitrogen gas. To this end we have examined C_2H_2 spectra using a hard collision Rautian profile over a range of five temperatures (213–333 K) and five pressures (5–40 Torr). From these fits we have obtained the N_2 -broadening and narrowing coefficients of C_2H_2 and examined their temperature dependence. The experimentally measured narrowing coefficients have been used to estimate the nitrogen diffusion coefficients (D_{12}) and are presented within. The broadening coefficients and corresponding temperature dependence exponents have also been compared to that of calculations completed using a classical impact approach on an ab initio potential energy surface. We have observed good agreement between our theoretical and experimental results.

PACS Nos.: 33.20.-t, 33.20.Ea, 33.70.Jg, 32.70.Jz.

Résumé : Utilisant un spectromètre à diode laser à trois canaux, nous avons enregistré six transitions dans l'acétylène perturbée par de l'azote à l'intérieur de la bande d'absorption $\nu_1 + \nu_3$. Le but est d'améliorer notre compréhension des mécanismes d'élargissement et de resserrement dans l'acétylène à basse pression en présence d'azote. À cette fin, nous avons étudié les spectres de C_2H_2 en utilisant un profil de Rautian de collisions dures pour cinq températures dans le domaine 213–333 K et cinq pressions dans le domaine 5–40 Torr. À partir de ces ajustements numériques, nous avons obtenu les coefficients d'élargissement et de resserrement de C_2H_2 et avons examiné leur dépendance en température. Nous avons utilisé les valeurs obtenues expérimentalement pour les coefficients de resserrement afin d'estimer les coefficients de diffusion de l'azote (D_{12}) et nous les présentons ici. Les coefficients d'élargissement et la dépendance en température sont aussi comparés aux résultats de calculs qui utilisent une approche de collisions classiques et une surface d'énergie potentielle obtenue de principes premiers. Nous observons un bon accord entre calculs théoriques et valeurs expérimentales. [Traduit par la Rédaction]

1. Introduction

Accurate detailed knowledge of individual line parameters of the spectrum of acetylene is critical for the correct interpretation and modeling of many planetary atmospheres containing hydrocarbon molecules. The motivation behind this comes from our understanding that acetylene can be either a product or a reactant in many processes that are observed in planetary atmospheres [1–9]. Not only do we require good information about the self-interacting molecule, but we also require an intimate understanding of perturbed interactions. One of the most important perturbers we can examine is nitrogen as this is a major constituent of many atmospheres, such as Earth and Titan [7].

Table 1 shows a summary of the studies previously reporting on nitrogen-perturbed acetylene to date. From the table it is easy to see that most of our information has come from studies focused on room temperature measurements [10–20]. However, there have been a handful of studies that examined other temperature ranges [21–29]. It is the examination of these temperature dependencies that is vital to improving our interpretation of atmospheric data, as most regions of the atmosphere are not at a constant temperature. Therefore by obtaining temperature dependence exponents for broadening, shift, and narrowing we can

improve radiative transfer models used to examine data collected from remote sensing observations.

Our choice of the particular line shape of interest we want to examine is also vital to improving our understanding of these transitions. It has been found that the Voigt profile, though easy to fit, does not always obtain the most accurate results [12, 14, 16, 24, 25, 27–30]. This is even more important when considering low-pressure gas when collisional narrowing of the Doppler profile known as “Dicke narrowing” takes place [31]. The work presented here adopts the use of the hard collision Rautian line shape profile [32] to examine the temperature dependence of the N_2 -broadening and narrowing coefficients.

Present experimental measurements are compared to theoretical calculation of the collisional linewidths. The calculations presented here are the first ones performed for this system on a true potential energy surface (PES). Indeed, very recently [33] a four-dimensional ab initio PES has been determined for the $C_2H_2-N_2$ system. This PES has been computed using a supermolecular method in which the interaction energies are expressed as the difference between the energy of the complex and the energies of the monomers. Namely, the coupled cluster method at a single

Received 23 January 2013. Accepted 15 May 2013.

C. Povey and A. Predoi-Cross. Alberta Terrestrial Imaging Centre, Department of Physics and Astronomy, University of Lethbridge, 4401 University Drive, Lethbridge, AB T1K 3M4, Canada.
 M. Guilloré Obregon and F. Thibault. Institut de Physique de Rennes, UMR CNRS 6251, Université de Rennes I, F-35042 Rennes, France.
 S.V. Ivanov. Institute on Laser and Information Technologies, Russian Academy of Sciences, 2 Pionerskaya Str., 142190 Troitsk, Moscow, Russia.
 O.G. Buzykin. Central Aerohydrodynamic Institute (TsAGI), 140160 Zhukovski, Moscow Region, Russia.

Corresponding author: A. Predoi-Cross (e-mail: Adriana.predoi-cross@uleth.ca).

¹This manuscript is part of the special issue Mid- and Far-Infrared Spectroscopy: Techniques and Applications published in memoriam of our colleague Arvid Schultz.

Table 1. Summary of previous studies examining acetylene broadened by N₂.

Vibrational Band	Broadener	Temperatures (K)	Assignment range	Ref.
ν_5	N ₂ , O ₂	297	P(29)–R(25)	10
ν_5	N ₂ , O ₂	297	P(35)–R(34)	17
ν_5	H ₂ , N ₂ , He, Ar	147–295	P(8)–R(21)	21
ν_5	H ₂ , N ₂ , He, Ar	296	R(3)–R(34)	18
ν_5	N ₂	173.4	P(29)–R(28)	22
$\nu_4 + \nu_5 - \nu_4$	N ₂ , He	296	Q(1)–Q(35)	19
$2\nu_5 - \nu_5$	N ₂ , He	296	Q(1)–Q(35)	19
$\nu_4 + \nu_5 - \nu_4$	N ₂ , He	183.2–198.2	Q(1)–Q(35)	23
$2\nu_5 - \nu_5$	N ₂ , He	183.2–198.2	Q(1)–Q(35)	23
$\nu_4 + \nu_5$	N ₂ , air	296	P(31)–R(20)	11
$\nu_4 + \nu_5$	N ₂	173.2–273.2	P(1)–R(23)	24
$\nu_4 + \nu_5$	N ₂	298	P(17)–R(22)	12
$\nu_4 + \nu_5$	N ₂	173.2–298.2	R(11)–P(23)	25
$\nu_1 + \nu_3$	H ₂ , N ₂ , D ₂ , air	295	P(31)–R(27)	13
$\nu_1 + \nu_3$	C ₂ H ₂ , N ₂	296	P(11)	14
$\nu_1 + \nu_3$	N ₂	195, 373, 473	P(25)–R(25)	26
$\nu_1 + \nu_3$	N ₂ , O ₂ , CO ₂	296	P(26)–P(22)	20
$\nu_1 + \nu_3$	N ₂	213–333	P(31)–R(33)	28
$\nu_1 + \nu_5$	C ₂ H ₂ , N ₂ , Ar	296	R(0)–R(7), Q(7)–Q(29)	15
$\nu_1 + 3\nu_3$	N ₂ , O ₂ , He, Ar, Ne, Kr, Xe	298	P(17)–R(22)	16

and double excitations level with triple excitations included perturbatively (i.e., CCSD(T)) has been used.

2. Experimental details

All of the experimental data presented here were recorded using a three-channel tunable diode laser spectrometer at the University of Lethbridge. A description of the setup and its functionality can be found in ref. 27. The New Focus Velocity laser system provides a tunable range of 1.5 to 1.57 μm and can provide a signal-to-noise ratio better than 1000. This high signal-to-noise ratio has proven to be very useful when examining low-pressure spectra [29]. The radiation from the laser is directed through two sample chambers. The first is a temperature- and pressure-controlled chamber with a path length of 1.54 cm where the mixture of N₂ and C₂H₂ was filled. The second is a slightly smaller chamber with the same path length. This chamber was filled with pure gas at room temperature and used as a calibration source.

The spectra of six transitions (P(21), P(19), P(16), R(21), R(19), and R(16)) belonging to the $\nu_1 + \nu_3$ absorption band of acetylene were recorded. The gas used for the reference chamber was pure C₂H₂ provided by Praxair with a quoted concentration of 99.6%. The gas sample kept inside the temperature control chamber was also provided by Praxair and was quoted as being 9.94% C₂H₂ with the remaining being N₂. Low-pressure tests on the P(11) transition in the $\nu_1 + \nu_3$ band showed that the concentration was within 0.5% of the quoted value.

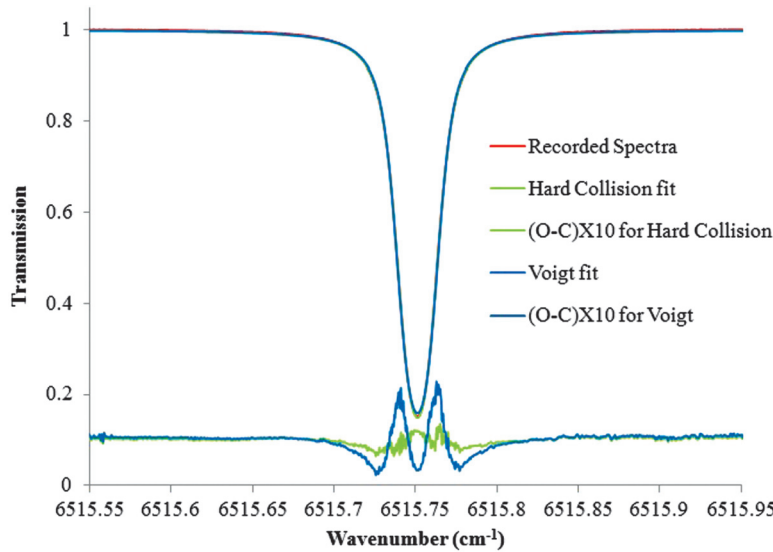
The spectra were recorded at the following temperatures: 213, 253, 296, 313, and 333 K. For each set temperature we recorded spectra at 40, 30, 20, 10, and 5 Torr. The temperature of the temperature-controlled chamber was monitored by an eight-channel Lakeshore (model 218) temperature monitor and controlled by a NesLab ULT 80 chiller. The gas sample pressures were monitored by two MKS Baratron capacitance manometers with full-scale reading of 10 and 100 Torr. The 10 Torr gauge was used for monitoring the gas pressures inside the reference chamber and the 100 Torr gauge was used to monitor the pressures inside the temperature-controlled chamber. Once thermal equilibrium was reached the sample temperatures and pressures were stable to within ±0.3 K and ±0.1% during the course of each scan [27, 29]. Table 2 shows the experimental details for the R(21) transition with the other five transitions having very similar pressures and temperatures.

Table 2. Sample of experimental conditions for the R(21) transition.

Temperature (K)	Pressure (Torr)	Number of recorded spectra
213.9(3)	5.214(5)	4
213.9(3)	10.214(10)	4
213.9(3)	20.270(20)	4
213.9(3)	30.408(30)	4
213.9(3)	42.371(42)	3
253.4(3)	5.267(5)	4
253.4(3)	10.668(11)	4
253.4(3)	20.131(20)	4
253.4(3)	30.185(30)	4
253.4(3)	40.409(40)	4
295.8(3)	5.264(5)	4
295.8(3)	10.324(10)	4
295.8(3)	19.839(20)	4
295.8(3)	30.013(30)	4
295.8(3)	40.364(40)	4
312.7(3)	5.170(5)	4
312.7(3)	10.250(10)	4
312.7(3)	19.910(20)	4
312.7(3)	30.087(30)	4
312.7(3)	39.286(39)	4
332.5(3)	5.499(5)	4
332.5(3)	10.898(11)	4
332.5(3)	21.153(21)	4
332.5(3)	29.983(30)	4
332.5(3)	40.022(40)	2

The recorded spectra were fit using a multispectral fitting routine [34]. This routine allows for simultaneous fitting of spectra at several different pressures for one set temperature. It also allows for the inclusion of an instrumental line shape (ILS), which is convolved with the spectral line shape of choice. To minimize any errors in our results we have used the same ILS as was previously discussed and verified in ref. 29. The experimental errors associated with the measured broadening and narrowing coefficients are assumed to have the same values as those discussed in ref. 29, where we found there to be an error no greater than 1% and 3% for our determined broadening and narrowing parameters, respec-

Fig. 1. Observed and calculated spectra for the P(16) transition of the $\nu_1 + \nu_3$ absorption band of C_2H_2 at a pressure of 40 Torr and temperature of 296 K. The residuals have been shifted and magnified for easier comparison.



tively. Initial parameters for both self- and N_2 -broadening, shift, and narrowing were obtained from refs. 28 and 29. The HITRAN database [35] was used for all line positions and intensities. Though not directly observed at the pressures measured here the effects due to line mixing were included within the fitting routine and were set to the values reported in ref. 27.

3. Spectroscopic line shape analysis

When fitting recorded laboratory spectra it becomes very important to choose the appropriate line shape function that will mimic the physical conditions of the gas under examination. Typically for remote sensing purposes we use a Voigt line shape function, which is a convolution of Lorentz and Doppler line shape functions. The Voigt profile is a fast and reliable way to examine spectra of this nature. However, with ever-improving advances in signal-to-noise ratio for new remote sensing instruments being developed, more subtle effects that were not noticeable in the past now influence the errors in our results.

One such effect is known as “Dicke narrowing”. This narrowing effect occurs at intermediate pressures when the mean free path of the molecules becomes equal to or less than the wavelength of the incident radiation. When this condition is met a simple Voigt profile will result in the retrieval of broadening coefficients that are smaller than we would expect to observe. To account for this narrowing we can adopt a line shape function that includes the mechanisms of the Dicke narrowing effect.

To account for such an effect, soft and hard collision models are often used [32, 36]. Despite the physics leading to these models being very different, it was found for the case of the self-perturbed spectrum of C_2H_2 [29] that there was no substantial difference in the residuals produced from fits of these two line shape functions to that of the experimental lineshape even though they did produce slightly different narrowing parameters. Generally, the choice of which line shape function to fit to the experimental lineshape comes down to the masses of the perturber and radiator, as was seen for the self-perturbed case [29] neither lineshape function was preferable. For the case of N_2 perturbed spectrum of C_2H_2 it was decided to only make use of an uncorrelated hard collision Rautian line shape function as the mass of N_2 and C_2H_2 are very similar. Therefore, fitting of the experimental lineshape function using the Galatry lineshape function was assumed to add no extra value to our analysis. Figure 1 shows the spectra of the

P(16) line of the $\nu_1 + \nu_3$ band measured at 40 Torr. In the figure one can see that when fitting with a Voigt profile we get a w-type residual, which is indicative of the broadening in the Dicke narrowing regime. It is clearly shown that once we fit the data using a diffusion profile, such as the Rautian, we get an improved result. It was found that for the spectra recorded at 333 K the percent difference between the obtained broadening coefficients using the Voigt and Rautian lineshape functions was as high as 6%. This difference in retrieved values diminished along with the temperature as we observed that at lower temperatures (i.e., 213 K) we had only 3% difference.

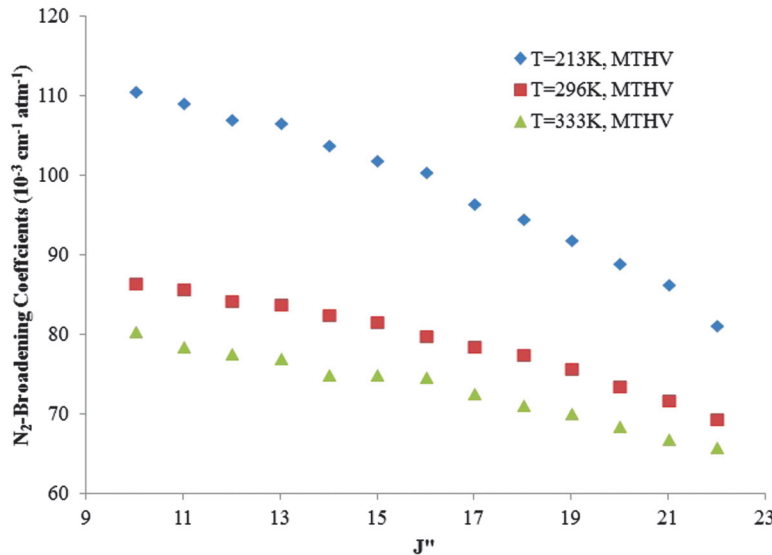
We present the expressions used to retrieve the N_2 -broadened half-width and narrowing coefficients temperature dependences

$$\gamma(p, T) = p \left[\gamma_{\text{N}_2}^{\text{o}}(p_o, T_o)(1 - \chi) \left(\frac{T_o}{T} \right)^{n_1} + \gamma_{\text{self}}^{\text{o}}(p_o, T_o)\chi \left(\frac{T_o}{T} \right)^{n_2} \right] \quad (1)$$

$$\beta(p, T) = p \left[\beta_{\text{N}_2}^{\text{o}}(p_o, T_o)(1 - \chi) \left(\frac{T_o}{T} \right)^{n'_1} + \beta_{\text{self}}^{\text{o}}(p_o, T_o)\chi \left(\frac{T_o}{T} \right)^{n'_2} \right] \quad (2)$$

In (1) and (2) the reference pressure and temperature are $p_o = 1 \text{ atm}$ and $T_o = 296 \text{ K}$, respectively; $\gamma_{\text{N}_2}^{\text{o}}$ and $\beta_{\text{N}_2}^{\text{o}}$ are the retrieved N_2 -broadened half-width and narrowing coefficients at the reference pressure, p_o (1 atm), and reference temperature, T_o (296 K); γ and β are the measured broadened half-width and narrowing coefficients, respectively, of the spectral line at the total sample pressure, p , and temperature, T ; the total sample pressure $p = p_{\text{N}_2} + p_{\text{self}}$; χ is the ratio of p_{self} to p ; and n and n' are the temperature dependence exponents of the broadened half-width and narrowing coefficients, respectively. The use of (2) for examining the temperature dependence of the narrowing coefficient has been justified by the work of both Li et al. [37, 38] and Povey et al. [29]. It is important to note that (1) and (2) are merely approximations that will become less valid with increasing temperatures [39].

Using a hard collision Rautian line shape model we have examined the N_2 -broadening and narrowing parameters for six transitions in the $\nu_1 + \nu_3$ band of C_2H_2 . The line parameters were obtained using a weighted multispectrum analysis software [34]. For one set temperature multispectrum fits were performed on the set of spectra recorded for different pressures. The software uses a nonlinear fitting routine to optimize the line parameters by minimizing the residual.

Fig. 2. Classically calculated pressure broadening coefficients at the 3 temperatures studied.**Table 3.** N₂-broadening coefficients for five different temperatures obtained using an uncorrelated hard collision Rautian line shape model. Retrieved N₂-broadening coefficients $\gamma_{N_2}^o$ (cm⁻¹ atm⁻¹).

Line	m	Line Position (cm ⁻¹)	213 K	253 K	296 K	313 K	333 K
P(21)	-21	6501.7047	0.0888(9)	0.0798(8)	0.0708(7)	0.0692(7)	0.0665(7)
P(19)	-19	6507.3982	0.0947(9)	0.0832(8)	0.0769(8)	0.0719(7)	0.0704(7)
P(16)	-16	6515.7516	0.1017(10)	0.0889(9)	0.0774(8)	0.0766(8)	0.0714(7)
R(16)	17	6592.5030	0.0985(10)	0.085(9)	0.0752(8)	0.0727(7)	0.0699(7)
R(19)	20	6598.0774	0.0913(9)	0.0823(8)	0.0739(7)	0.0725(7)	0.0673(7)
R(21)	22	6601.6617	0.0859(9)	0.0768(8)	0.0693(7)	0.0689(7)	0.0676(7)

Note: The normal convention of $m = -J''$ for the P branch and $m = J'' + 1$ for the R branch is used.

For each line examined a simultaneous fit of the intensity, N₂-broadening and -narrowing was completed. The shift was also fit simultaneously, however, because of the low pressures of the sample gas, the results for the shift were not ideal for publication.

3.1. Modeled N₂-broadened line width

In this work we calculate the linewidths of C₂H₂ infrared spectral lines (electric dipole absorption) broadened by N₂ in the frames of the classical impact approach of Gordon [40, 41] for isolated lines (no pressure-induced interference). To model translational and rotational motion of C₂H₂ and N₂ molecules we use three-dimensional exact classical equations of motion that describe the collision of two rigid linear molecules.

The dynamics were performed on the four-dimensional ab initio PES of Thibault et al. [33]. For technical (and computing) reasons this PES has been developed, from 2 to 21 Å, over 85 bispherical harmonics [42, 43]. Such a large expansion is required because of the steepness of the repulsive part of the potential at short range: a region of major importance for the calculations of pressure broadening coefficients for temperatures greater than about 100 K.

Classical calculations were done for three temperatures of the C₂H₂-N₂ mixture: 213, 296, and 333 K and are shown in Fig. 2. Exact classical three-dimensional dynamics of C₂H₂-N₂ collisions were described by 17 first-order Hamilton differential equations in body-fixed coordinates [44]. Spin statistical weights of perturbing N₂ molecules were taken into account in the usual way. The initial intermolecular distance was set large enough (15 Å) to exclude starting interaction between molecules. Other collision parameters (initial conditions for trajectory calculations) were selected

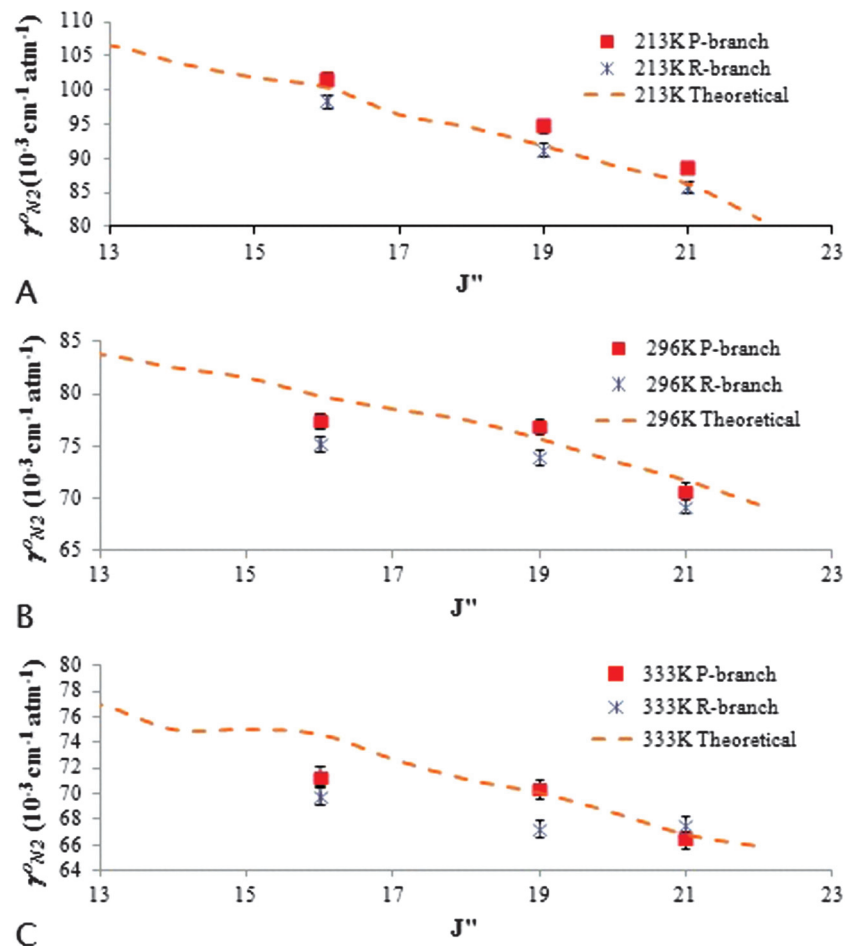
via a Monte Carlo procedure. Uniform sampling was applied to the directions of rotation and initial orientations of both molecules in three-dimensional space. A very effective algorithm of impact parameter b sampling [45] was used in Monte Carlo calculations, which reduces the computation time by half. The impact parameter was bracketed within the range of 0–12 Å. All the calculations were made using the approximation mean thermal velocity (MTHV), which greatly reduces CPU time. In the MTHV approximation all initial relative velocities of colliding molecules are set equal to their mean thermal relative velocity $\bar{v} = \sqrt{8k_B T/\pi\mu}$ associated with gas temperature (k_B being the Boltzmann constant and $\mu = 13.487$ u, μ being the reduced mass of the C₂H₂-N₂ pair). The statistical error of calculated linewidths (i.e., RMS error of Monte Carlo averaging over initial conditions of collisions) was kept for different values of temperature T and rotational quantum number J'' generally at a level less than 1%.

3.2. N₂-broadening of acetylene transitions

Table 3 shows the N₂-broadening coefficients measured for all five temperatures. A comparison of our experimental results with those of the theoretically determined line widths from Sect. 3.1 can be seen in Fig. 3. From the figure it can be seen that both sets of data agree quite well with a maximum relative difference no greater than 7%.

Figure 4 shows the results of our room temperature N₂-broadening coefficients and a comparison with previous measurements reported in the literature. As can be seen in the figure the linewidths that were retrieved in this study agree reasonably well with most of the previous work completed to date.

Fig. 3. Comparison of classically calculated and experimentally determined N₂-broadening coefficients for three different temperatures. In each panel the line depicts the theoretically determined broadening coefficients.



Using (1) we have calculated the temperature dependence of the N₂-broadening coefficients. Both experimentally and theoretically determined N₂-broadening temperature dependence coefficients, n , are shown in Table 4 and plotted in Fig. 5. In Fig. 5 we compare our current results with those found by Rozario et al. [28] and Campbell et al. [26]. Our coefficients of line broadening temperature dependence, n , reasonably match previous work done for larger values of the quantum number $|m|$. We immediately notice that as $|m|$ becomes smaller we have more deviation from both the theoretical work presented in this paper and that of Campbell et al. [26]. However, it is important to note that the work done by Campbell et al. [26] where they have smoothed out their results agrees quite well with the proposed theoretical calculations presented here. From Fig. 5 it can be seen that for the R-branch transitions we have much better agreement than we get for the P-branch transitions. It is our belief that the initial parameters used for the self-narrowing obtained from ref. 29 have allowed for less error to be introduced into the results obtained for the R-branch transitions. However, for the P-branch transitions we had to make the assumption that initial self-narrowing coefficients were similar to those obtained for the R-branch. At this moment we don't know of any published work showing both the m and temperature dependence of the self-narrowing coefficients for P-branch transitions.

3.3. N₂-narrowing of acetylene transitions

In our previous study [29] we determined that only transitions recorded at pressures below 40 Torr were strictly in the Dicke nar-

rowing regime. Therefore only spectra recorded at 40 Torr and below were recorded for this analysis. Figure 6 shows the relationship of the pressure-dependent narrowing coefficient for the P(16) line of the $v_1 + v_3$ band at 296 K plotted against the N₂ partial pressure of the chamber. It is clear from the figure that we have a linear relationship with pressure. This justifies our examination of the narrowing effects in this pressure region.

Table 5 shows the N₂-narrowing coefficients obtained from fitting the lineshape with the hard collision Rautian profile. The room temperature N₂-narrowing coefficients from Table 4 are compared in Fig. 7 to the values obtained for both self- and N₂-narrowing by Povey et al. [29], McRaven et al. [14], Dhyne et al. [24, 25], and Valipour and Zimmermann [16]. From the figure we see that all studies report similar results. Each of the previous studies that examined both self- and N₂-narrowing [14, 16] report the N₂-narrowing coefficients to be smaller than the self-narrowing coefficients. This is what we also observe when we compare our previous work [29] with the present results.

The exponents n'_1 for temperature dependence of N₂-narrowing are given in Table 5. These temperature dependence coefficients are plotted in Fig. 8 along with self-narrowing temperature dependence coefficients from ref. 29. From the figure it can be seen that the obtained temperature dependence is very similar and for the most part they agree to within one standard deviation.

3.4. Diffusion coefficients

Based on our previous study [29] we have equated the narrowing parameter, $\beta_{N_2}^0$, to the dynamic friction coefficient, β_{diff}^0 , in an

Fig. 4. Panel A shows a comparison of the present N₂-broadening coefficients with previous studies. Panel B shows a smaller region between $m = 10$ and 25 where only values obtained from a narrowing model are compared.

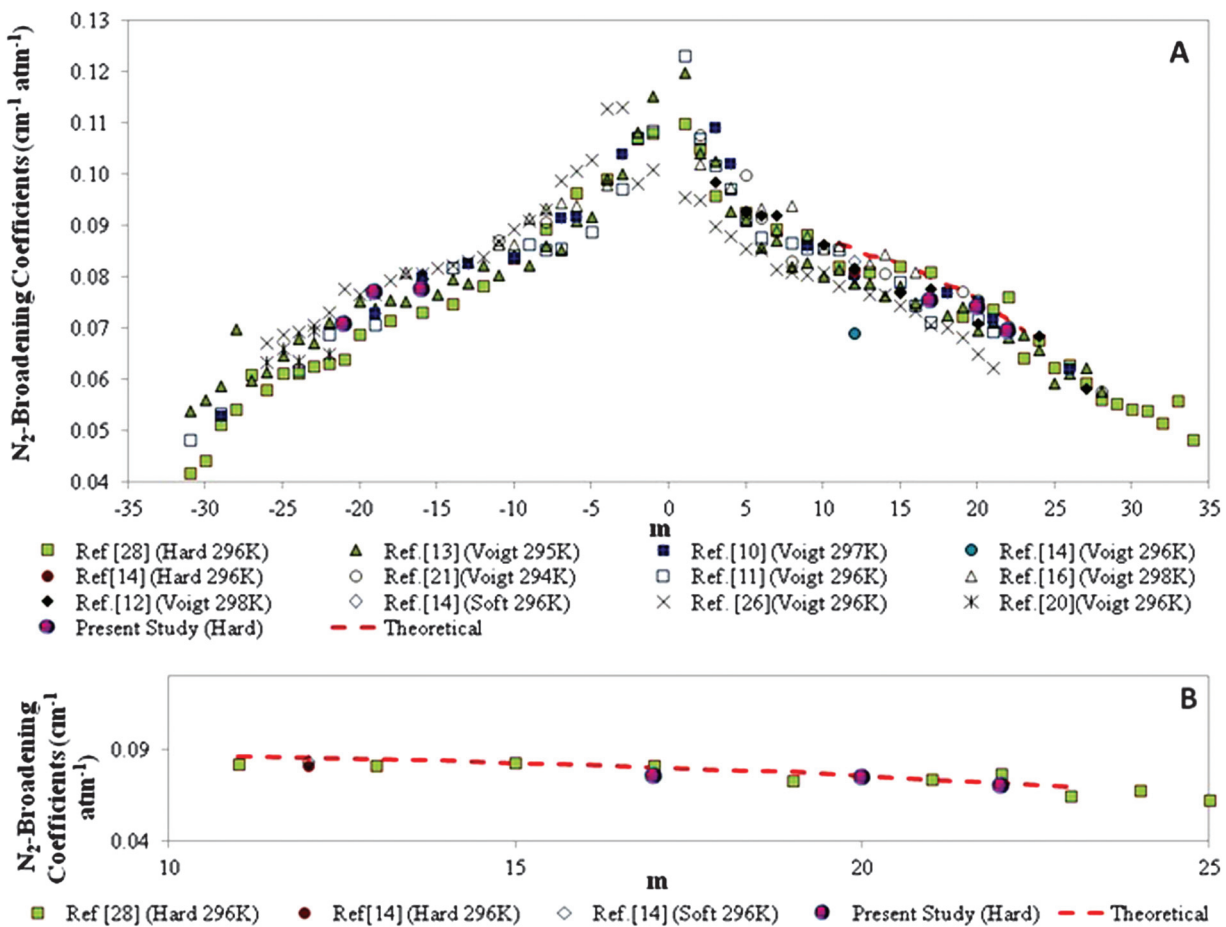


Table 4. Comparison of theoretical and experimental results obtained for N₂-broadening coefficients at 296 K and temperature dependence exponents n_1 . Retrieved N₂-broadening coefficients (cm⁻¹ atm⁻¹) at 296 K and determined temperature dependence exponents.

Line	m	Rautian $\gamma_{N_2}^0$	Calculated $\gamma_{N_2}^0$	% difference	Rautian n_1	Calculated n_1	% difference
P(21)	-21	0.0708(7)	0.0736	3.77	0.66(2)	0.57	12.87
P(19)	-19	0.0769(8)	0.0775	0.80	0.67(4)	0.60	9.30
P(16)	-16	0.0774(8)	0.0815	5.02	0.78(4)	0.67	13.66
R(16)	17	0.0752(8)	0.0798	5.73	0.77(2)	0.67	12.94
R(19)	20	0.0739(7)	0.0757	2.35	0.66(4)	0.60	7.97
R(21)	22	0.0693(7)	0.0717	3.37	0.55(5)	0.57	3.35

attempt to estimate the nitrogen diffusion coefficient and its temperature dependence. The dynamic friction coefficient, β_{diff}^0 , can be expressed by the following equation [37, 46]:

$$\beta_{\text{diff}}^0 = \frac{k_B T}{2\pi m c D_{12}} \quad (3)$$

where k_B is the Boltzmann constant, T is the temperature in kelvin, m is the mass of acetylene molecule, c is the speed of light, and D_{12} is the nitrogen diffusion coefficient for acetylene.

The mass diffusion coefficient for a gas mixture can be estimated in a general sense using the following equation [47, 48]:

$$D_{12} = \frac{\varepsilon_D k_B^{3/2}}{\sqrt{\pi p \sigma_{12}^2 \Omega_{12}^{(1,1)}(T_{12})}} \sqrt{\frac{(M_1 + M_2)}{2M_1 M_2}} \quad (4)$$

where M_1 and M_2 are the molecular weights of C₂H₂ and N₂, respectively; T is the temperature in kelvin; p is the pressure in atmospheres; $\varepsilon_D = 3/8$ as shown in [47]; T_{12} is a reduced temperature equal to $k_B T / \varepsilon_{12}$; ε_{12} is the depth of the isotropic potential; and σ_{12} is the finite distance at which the intermolecular isotropic potential is zero. From the ab initio PES [33], values of $\varepsilon_{12} = 88.8$ cm⁻¹ and $\sigma_{12} = 4.015$ Å were deduced and used. Finally, $\Omega_{12}^{(1,1)}$ is a dimensionless reduced collision integral, a function of the reduced temperature; values are tabulated in ref. 47.

Fig. 5. Temperature dependence exponents, n_1 , obtained from (1).

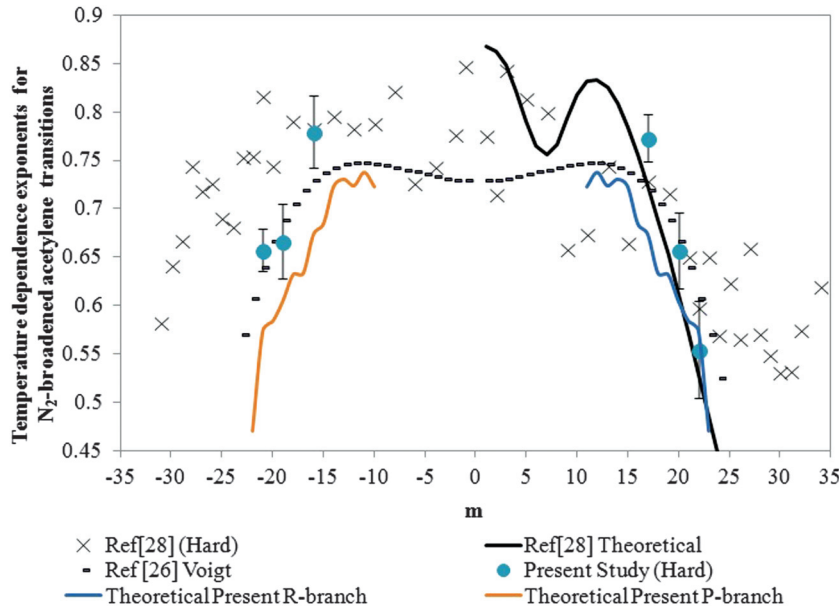
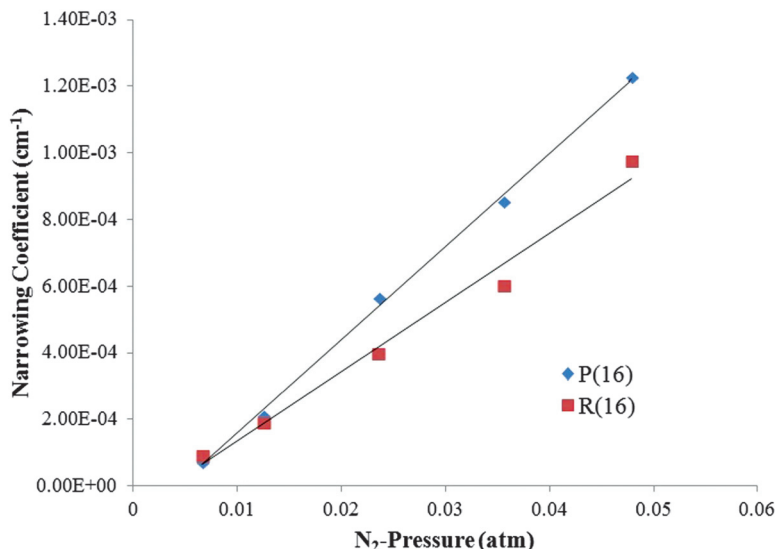


Fig. 6. The pressure-dependent narrowing coefficients, β_{N_2} , for the P(16) and R(16) transitions at 296 K as they vary with the partial N_2 pressure.



Using our obtained $\beta_{N_2}^0$ narrowing coefficients in (3) we calculated D_{12} for all the temperatures examined and have presented them in Table 6. The temperature dependence of the nitrogen diffusion coefficient was determined using (4) and was plotted in Fig. 9. A comparison of the experimentally estimated, through (3), nitrogen diffusion coefficients to those obtained using (4) shows a similar trend in the temperature dependence of the nitrogen diffusion coefficients. However, unlike in our previous work [29] where it was determined that our diffusion coefficients were slightly lower than those obtained theoretically, we see that now our values are slightly larger than those found using equation (4). This result indicates that $\beta_{\text{diff}}^0 > \beta_{N_2}^0$, which implies that we found less narrowing than expected on the basis $\beta_{\text{diff}}^0 = \beta_{N_2}^0$. Such a result was also found in the work done by Wehr et al. [49] for the CO-Ar system. We also should expect to see that for the P- and R-branch transitions the diffusion coefficients are similar (for a given m or

J'' value). In Fig. 9 we do in fact see this for the P(21) and R(21) transitions. The fact that we do not see as close agreement between the P(16) and R(16) as well as the P(19) and R(19) may in fact be due to neighboring spectral features that are not properly accounted for as there are many weak transitions in this spectral region. However, it does indicate the need for a closer examination of both self- and N_2 -narrowing coefficients for both P- and R-branch transitions on a larger scale than that presented here.

Moreover, our comparison between the binary diffusion coefficients as given by (4) and our effective (or optical) diffusion coefficient retrieved by our lineshape analysis cannot be completely satisfactory for the following reasons. First, but this is not the main reason, (4) is a first order approximation [47, 50]. Secondly, paraphrasing Varghese and Hanson [51] “the two parameters (the mass diffusion constant and the effective diffusion coefficient) appear in different contexts in the theory and hence do not have

Table 5. N₂-narrowing coefficients for the five recorded temperatures using an uncorrelated hard collision Rautian line shape model. Retrieved N₂-narrowing coefficients $\beta_{N_2}^0$ (cm⁻¹ atm⁻¹) and temperature dependence, n'_1 .

Line	m	213 K	253 K	296 K	313 K	333 K	n'_1
P(21)	-21	0.0279(9)	0.0225(7)	0.0182(6)	0.0177(6)	0.017(5)	1.146(78)
P(19)	-19	0.0273(9)	0.0232(7)	0.0184(6)	0.018(6)	0.0173(6)	1.076(81)
P(16)	-16	0.0256(8)	0.0239(8)	0.0217(7)	0.021(7)	0.0203(6)	0.533(26)
R(16)	17	0.0212(7)	0.0186(6)	0.0165(5)	0.0157(5)	0.015(5)	0.773(9)
R(19)	20	0.0211(7)	0.0188(6)	0.017(5)	0.016(5)	0.0153(5)	0.721(29)
R(21)	22	0.0225(7)	0.0209(7)	0.0187(6)	0.0173(6)	0.0163(5)	0.719(82)

Note: The last column shows the temperature dependence terms obtained from the data in the table and (2).

Fig. 7. Comparison of the N₂-narrowing coefficients obtained at 296 K to previous work.

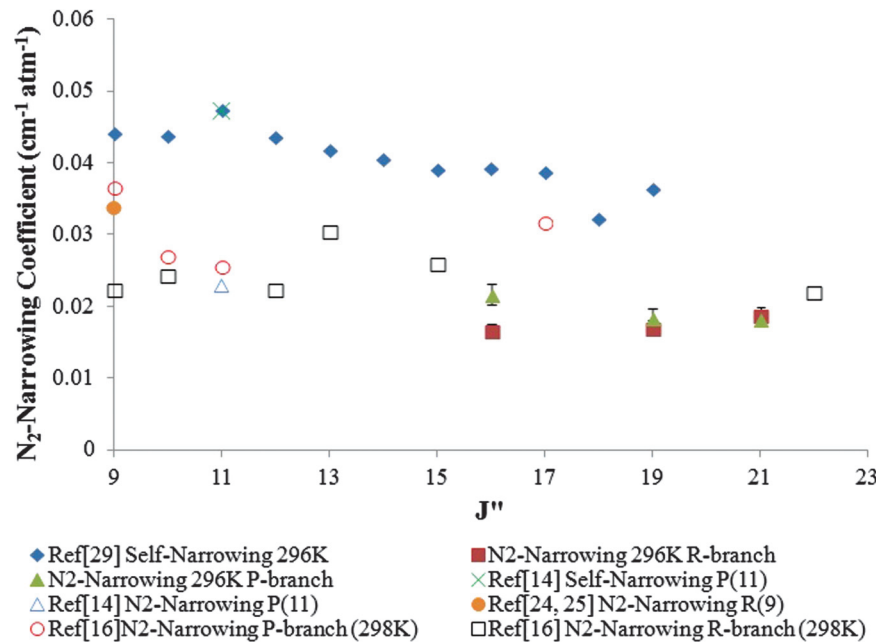


Fig. 8. Narrowing temperature dependence coefficient n'_1 obtained from (2). The diamonds show the results from our previous work [29] with self-narrowing coefficients.

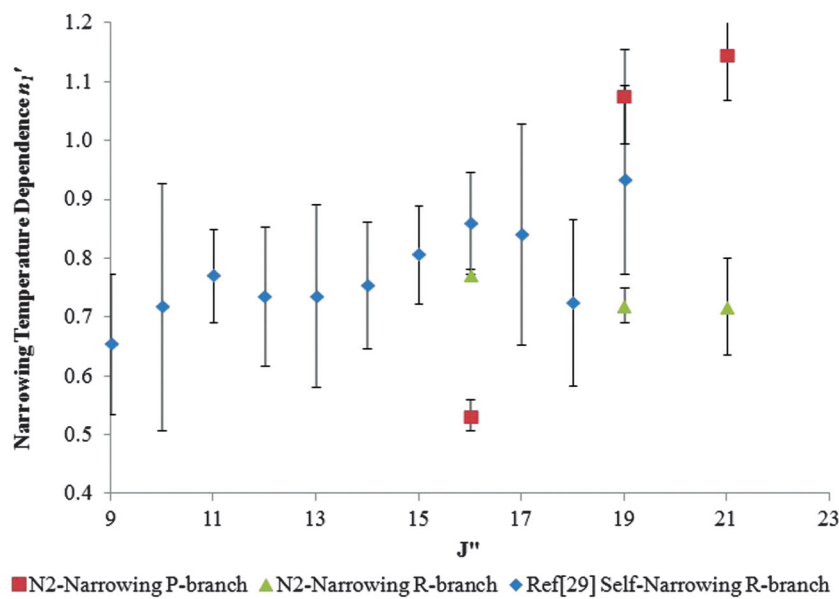
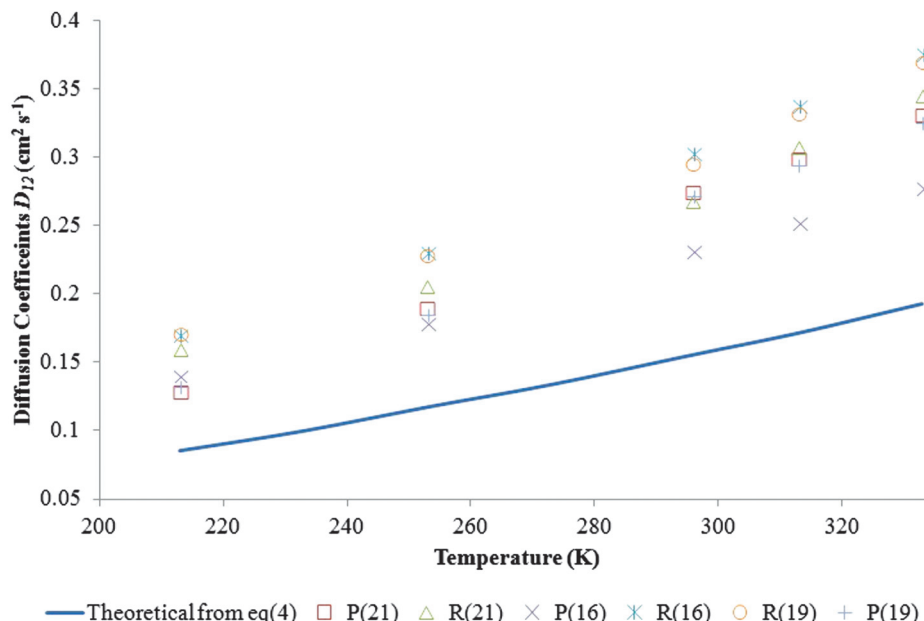


Table 6. Estimated N₂-diffusion coefficients obtained from (3). Retrieved N₂-diffusion coefficients D_{12} (cm² s⁻¹).

Line	m	213 K	253 K	296 K	% difference ^a	313 K	333 K
P(21)	-21	0.129(4)	0.190(6)	0.275(9)	43.37	0.300(10)	0.331(11)
P(19)	-19	0.132(4)	0.185(6)	0.272(9)	42.74	0.295(9)	0.326(10)
P(16)	-16	0.141(5)	0.179(6)	0.232(7)	32.77	0.253(8)	0.278(9)
R(16)	17	0.170(5)	0.231(7)	0.304(10)	48.73	0.338(11)	0.376(12)
R(19)	20	0.171(5)	0.228(7)	0.295(9)	47.22	0.332(11)	0.370(12)
R(21)	22	0.160(5)	0.206(7)	0.268(9)	41.82	0.307(10)	0.345(11)

^aFor the values obtained at 296 K a percent difference was calculated (theoretical – experimental)/experimental.

Fig. 9. Estimated diffusion coefficients obtained from retrieved experimental $\beta_{N_2}^0$ and (4).

the same physical significance...". More recently, Wehr et al. [49] have also pointed out that both coefficients are related to (or take into account) different collisional mechanisms (in addition, many studies found large discrepancies between these two kinds of coefficients, see references in ref. 49). Therefore, one can only expect rough agreement between these coefficients and such spectroscopic analysis can only provide an order of magnitude for the true binary diffusion coefficient.

4. Conclusion

Using a three-channel tunable diode laser system we have for the first time examined the temperature dependence of N₂-narrowing coefficients for six transitions in the $v_1 + v_3$ absorption band of acetylene. The N₂-broadening that was obtained while examining the hard collision Rautian line shape profile agrees very well with the theoretical calculations presented here. The full classical values calculated on the very first complete four-dimension ab initio PES [33] for the C₂H₂-N₂ system are very encouraging and will allow us to compare the methods for determining pressure broadening coefficients for this system, as was recently done for similar systems (N₂-H₂, N₂-N₂, C₂H₂-H₂, see refs. 52–54). In addition, careful comparisons of both our N₂-broadening and narrowing coefficients with previous studies have shown strong agreement.

For a more physical interpretation of the narrowing effects in our low-pressure spectra we should consider two main effects. The first one is the Dicke narrowing effect discussed in detail in this study. The second contribution to line narrowing arises from the effects of molecular speed dependence on collisional line

broadening. Using our software we were unable to quantify individual contributions to line narrowing. Any analysis that takes into account both Dicke narrowing and speed-dependent collisional broadening would have to be done carefully to avoid any fitting error due to the highly correlated nature of these two effects.

Acknowledgements

This work was supported by the Natural Sciences and Engineering Research Council of Canada. We would like to further thank the AMETHYST program at the University of Lethbridge for their continued funding and academic support. We are grateful to D.R. Hurtmans of Universite Libre de Bruxelles for making available to us his line shape fitting software. Finally CP would like to thank his father, R. Povey (who passed away during the writing of this document) for his long-time support and guidance.

References

1. H.W. Moos and J.T. Clarke. ApJ, **229**, L107 (1979). doi:[10.1086/182939](https://doi.org/10.1086/182939).
2. D. Cronn and E. Robinson. Geophys. Res. Lett. **6**, 641 (1979). doi:[10.1029/GL006i008p00641](https://doi.org/10.1029/GL006i008p00641).
3. A. Goldman, F.J. Murcray, R.D. Blatherwick, J.R. Gillis, F.S. Bonomo, F.H. Murcray, D.G. Murcray, and R.J. Cicerone. J. Geophys. Res.-Oceans Atmos. **86**, 2143 (1981). doi:[10.1029/JA086iA04p02143](https://doi.org/10.1029/JA086iA04p02143).
4. R. Zander, C.P. Rinsland, D.H. Ehhalt, J. Rudolph, and P. Demoulin. J. Atmos. Chem. **13**, 359 (1991). doi:[10.1007/BF00057752](https://doi.org/10.1007/BF00057752).
5. J. Rudolph, A. Khedim, and B. Bonsang. J. Geophys. Res. D: Atmos. **97**, 6181 (1992). doi:[10.1029/91JD00289](https://doi.org/10.1029/91JD00289).
6. T. Fouchet, E. Lellouch, B. Bezard, H. Feuchtgruber, P. Drossart, and T. Encrenaz. Astron. Astrophys. **355**, L13 (2000).
7. A. Coustenis, et al. Icarus, **189**, 35 (2007). doi:[10.1016/j.icarus.2006.12.022](https://doi.org/10.1016/j.icarus.2006.12.022).

8. T. Kostiuk, et al. *Planet. Space Sci.* **58**, 1715 (2010). doi:[10.1016/j.pss.2010.08.004](https://doi.org/10.1016/j.pss.2010.08.004).
9. C.A. Nixon, R.K. Achterberg, P.N. Romani, M. Allen, X. Zhang, N.A. Teamby, P.G.J. Irwin, and F.M. Flasar. *Planet. Space Sci.* **58**, 1667 (2010). doi:[10.1016/j.pss.2010.05.008](https://doi.org/10.1016/j.pss.2010.05.008).
10. D. Lambot, G. Blanquet, and J.P. Bouanich. *J. Mol. Spectrosc.* **136**, 86 (1989). doi:[10.1016/0022-2852\(89\)90221-X](https://doi.org/10.1016/0022-2852(89)90221-X).
11. V.M. Devi, D.C. Benner, C.P. Rinsland, M.A.H. Smith, and B.D. Sidney. *J. Mol. Spectrosc.* **114**, 49 (1985). doi:[10.1016/0022-2852\(85\)90335-2](https://doi.org/10.1016/0022-2852(85)90335-2).
12. L. Fissiaux, M. Dhyne, and M. Lepere. *J. Mol. Spectrosc.* **254**, 10–15 (2009).
13. S.W. Arteaga, et al. *J. Mol. Spectrosc.* **243**, 253 (2007). doi:[10.1016/j.jms.2007.04.007](https://doi.org/10.1016/j.jms.2007.04.007).
14. C.P. McRaven, M.J. Cich, G.V. Lopez, T.J. Sears, D. Hurtmans, and A.W. Mantz. *J. Mol. Spectrosc.* **266**, 43 (2011). doi:[10.1016/j.jms.2011.02.016](https://doi.org/10.1016/j.jms.2011.02.016).
15. A.S. Pine. *J. Quant. Spectrosc. Radiat. Transfer*, **50**, 149 (1993). doi:[10.1016/0022-4073\(93\)90114-W](https://doi.org/10.1016/0022-4073(93)90114-W).
16. H. Valipour and D. Zimmermann. *J. Chem. Phys.* **114**, 3535 (2001). doi:[10.1063/1.1333022](https://doi.org/10.1063/1.1333022).
17. J.P. Bouanich, D. Lambot, G. Blanquet, and J. Walrand. *J. Mol. Spectrosc.* **140**, 195 (1990). doi:[10.1016/0022-2852\(90\)90134-C](https://doi.org/10.1016/0022-2852(90)90134-C).
18. A. Babay, M. Ibrahim, V. Lemaire, B. Lemoine, F. Rohart, and J.P. Bouanich. *J. Quant. Spectrosc. Radiat. Transfer*, **59**, 195 (1998). doi:[10.1016/S0022-4073\(97\)00122-2](https://doi.org/10.1016/S0022-4073(97)00122-2).
19. J.P. Bouanich, G. Blanquet, and J. Walrand. *J. Mol. Spectrosc.* **203**, 41 (2000). doi:[10.1006/jmsp.2000.8160](https://doi.org/10.1006/jmsp.2000.8160). PMID:[10930331](#).
20. P. Minutolo, C. Corsi, F. D'Amato, and M. De Rosa. *Eur. Phys. J. D*, **17**, 175 (2001). doi:[10.1007/s100530100200](https://doi.org/10.1007/s100530100200).
21. P. Varanasi. *J. Quant. Spectrosc. Radiat. Transfer*, **47**, 263 (1992). doi:[10.1016/0022-4073\(92\)90145-T](https://doi.org/10.1016/0022-4073(92)90145-T).
22. J.P. Bouanich, G. Blanquet, J.C. Populaire, and J. Walrand. *J. Mol. Spectrosc.* **190**, 7 (1998). doi:[10.1006/jmsp.1998.7559](https://doi.org/10.1006/jmsp.1998.7559). PMID:[9645924](#).
23. G. Blanquet, J. Walrand, and J.P. Bouanich. *J. Mol. Spectrosc.* **210**, 1 (2001). doi:[10.1006/jmsp.2001.8441](https://doi.org/10.1006/jmsp.2001.8441).
24. M. Dhyne, L. Fissiaux, J.C. Populaire, and M. Lepere. *J. Quant. Spectrosc. Radiat. Transfer*, **110**, 358 (2009). doi:[10.1016/j.jqsrt.2008.12.009](https://doi.org/10.1016/j.jqsrt.2008.12.009).
25. M. Dhyne, P. Joubert, J.C. Populaire, and M. Lepere. *J. Quant. Spectrosc. Radiat. Transfer*, **111**, 973 (2010). doi:[10.1016/j.jqsrt.2009.12.004](https://doi.org/10.1016/j.jqsrt.2009.12.004).
26. N.T. Campbell, et al. *Mol. Phys.* **109**, 2199 (2011). doi:[10.1080/00268976.2011.609139](https://doi.org/10.1080/00268976.2011.609139).
27. C. Povey, A. Predoi-Cross, and D.R. Hurtmans. *J. Mol. Spectrosc.* **268**, 177 (2011). doi:[10.1016/j.jms.2011.04.020](https://doi.org/10.1016/j.jms.2011.04.020).
28. H. Rozario, J. Garber, C. Povey, D. Hurtmans, J. Buldyрева, and A. Predoi-Cross. *Mol. Phys.* **110**, 2645 (2012). doi:[10.1080/00268976.2012.720040](https://doi.org/10.1080/00268976.2012.720040).
29. C. Povey, A. Predoi-Cross, and D.R. Hurtmans. *Mol. Phys.* **110**, 2633 (2012). doi:[10.1080/00268976.2012.705908](https://doi.org/10.1080/00268976.2012.705908).
30. F. Herregodts, D. Hurtmans, J. Vander Auwera, and M. Herman. *J. Chem. Phys.* **111**, 7954 (1999). doi:[10.1063/1.480129](https://doi.org/10.1063/1.480129).
31. R.H. Dicke. *Phys. Rev.* **89**, 472 (1953). doi:[10.1103/PhysRev.89.472](https://doi.org/10.1103/PhysRev.89.472).
32. S.G. Rautian and I.I. Sobelman. *Soviet Physics Uspekhi-Ussr*, **9**, 701 (1967). doi:[10.1070/PU1967v009n05ABEH003212](https://doi.org/10.1070/PU1967v009n05ABEH003212).
33. F. Thibault, O. Vieuxmaire, T. Sizun, and B. Bussery-Honvault. *Mol. Phys.* **110**, 2761 (2012). doi:[10.1080/00268976.2012.718380](https://doi.org/10.1080/00268976.2012.718380).
34. D. Hurtmans, G. Dufour, W. Bell, A. Henry, A. Valentini, and C. Camy-Peyret. *J. Mol. Spectrosc.* **215**, 128 (2002). doi:[10.1006/jmsp.2002.8620](https://doi.org/10.1006/jmsp.2002.8620).
35. L.S. Rothman, et al. *J. Quant. Spectrosc. Radiat. Transfer*, **110**, 533 (2009). doi:[10.1016/j.jqsrt.2009.02.013](https://doi.org/10.1016/j.jqsrt.2009.02.013).
36. L. Galatry. *Phys. Rev.* **122**, 1218 (1961). doi:[10.1103/PhysRev.122.1218](https://doi.org/10.1103/PhysRev.122.1218).
37. H. Li, A. Farooq, J.B. Jeffries, and R.K. Hanson. *Appl. Phys. B: Lasers Optics*, **89**, 407 (2007). doi:[10.1007/s00340-007-2781-9](https://doi.org/10.1007/s00340-007-2781-9).
38. H. Li, A. Farooq, J.B. Jeffries, and R.K. Hanson. *J. Quant. Spectrosc. Radiat. Transfer*, **109**, 132 (2008). doi:[10.1016/j.jqsrt.2007.05.008](https://doi.org/10.1016/j.jqsrt.2007.05.008).
39. J. Bonamy, D. Robert, and C. Boulet. *J. Quant. Spectrosc. Radiat. Transfer*, **31**, 23 (1984). doi:[10.1016/0022-4073\(84\)90046-3](https://doi.org/10.1016/0022-4073(84)90046-3).
40. R.G. Gordon. *J. Chem. Phys.* **44**, 3083 (1966). doi:[10.1063/1.1727183](https://doi.org/10.1063/1.1727183).
41. R.G. Gordon. *J. Chem. Phys.* **45**, 1649 (1966). doi:[10.1063/1.1727808](https://doi.org/10.1063/1.1727808).
42. L. Gomez, R.Z. Martinez, D. Bermejo, F. Thibault, P. Joubert, B. Bussery-Honvault, and J. Bonamy. *J. Chem. Phys.* **126**, (2007).
43. F. Thibault, B. Corretja, A. Viel, D. Bermejo, R.Z. Martinez, and B. Bussery-Honvault. *Phys. Chem. Chem. Phys.* **10**, 5419 (2008). doi:[10.1039/b804306j](https://doi.org/10.1039/b804306j). PMID:[18766239](#).
44. S.V. Ivanov and O.G. Buzykin. *Mol. Phys.* **106**, 1291 (2008). doi:[10.1080/00268970802270034](https://doi.org/10.1080/00268970802270034).
45. S. Chapman and S. Green. *J. Chem. Phys.* **67**, 2317 (1977). doi:[10.1063/1.435067](https://doi.org/10.1063/1.435067).
46. M. Lepere, A. Henry, A. Valentini, and C. Camy-Peyret. *J. Mol. Spectrosc.* **208**, 25 (2001). doi:[10.1006/jmsp.2001.8372](https://doi.org/10.1006/jmsp.2001.8372). PMID:[11437549](#).
47. J.O. Hirschfelder, C.F. Curtiss, and R.B. Bird. *The Molecular Theory of Gases and Liquids*. Wiley-Interscience, 1964. pp. 1280.
48. F. Thibault, A.W. Mantz, C. Claveau, A. Henry, A. Valentini, and D. Hurtmans. *J. Mol. Spectrosc.* **246**, 118 (2007). doi:[10.1016/j.jmsp.2007.09.001](https://doi.org/10.1016/j.jmsp.2007.09.001).
49. R. Wehr, R. Ciurylo, A. Vitcu, F. Thibault, J.R. Drummond, and A.D. May. *J. Mol. Spectrosc.* **235**, 54 (2006). doi:[10.1016/j.jmsp.2005.10.009](https://doi.org/10.1016/j.jmsp.2005.10.009).
50. F.R.W. McCourt, J.J.M. Beenaker, W.E. Köhler, and I. Kučšer. *Non equilibrium phenomena in polyatomic gases*. Clarendon Press, Oxford, 1990.
51. P.L. Varghese and R.K. Hanson. *Appl. Opt.* **23**, 2376 (1984). doi:[10.1364/AO.23.002376](https://doi.org/10.1364/AO.23.002376). PMID:[18213005](#).
52. F. Thibault, S.V. Ivanov, O.G. Buzykin, L. Gomez, M. Dhyne, P. Joubert, and M. Lepere. *J. Quant. Spectrosc. Radiat. Transfer*, **112**, 1429 (2011). doi:[10.1016/j.jqsrt.2011.02.011](https://doi.org/10.1016/j.jqsrt.2011.02.011).
53. L. Gomez, S.V. Ivanov, O.G. Buzykin, and F. Thibault. *J. Quant. Spectrosc. Radiat. Transfer*, **112**, 1942 (2011). doi:[10.1016/j.jqsrt.2011.04.005](https://doi.org/10.1016/j.jqsrt.2011.04.005).
54. F. Thibault, L. Gomez, S.V. Ivanov, O.G. Buzykin, and C. Boulet. *J. Quant. Spectrosc. Radiat. Transfer*, **113**, 1887 (2012). doi:[10.1016/j.jqsrt.2012.06.003](https://doi.org/10.1016/j.jqsrt.2012.06.003).